# Measuring $^{13}C$-enriched $CO_2$ in air with a cavity ring-down spectroscopy gas analyser: Evaluation and calibration

Dane Dickinson[1*], Samuel Bodé[2], Pascal Boeckx[2]

[1] Biosystems Engineering, Ghent University, Coupure Links 653, 9000 Gent, Belgium

[2] Isotope Bioscience Laboratory – ISOFYS, Ghent University, Coupure Links 653, 9000 Gent, Belgium

[*] Correspondence to: dane.dickinson@ugent.be

**Keywords:** cavity ring-down spectroscopy, $\delta^{13}C$, $^{13}CO_2$, Picarro G2131-i, $^{13}C$-enrichment, CRDS



This article has been accepted for publication and undergone full peer review but has not been through the copyediting, typesetting, pagination and proofreading process which may lead to differences between this version and the Version of Record. Please cite this article as doi: 10.1002/rcm.7969

**Abstract**

**RATIONALE:** Cavity ring-down spectroscopy (CRDS) is becoming increasingly popular for $\delta^{13}C$-$CO_2$ analysis of air. However, little is known about the effect of high $^{13}C$ abundances on CRDS performance. Overlap between $^{12}CO_2$ and $^{13}CO_2$ spectral lines may adversely affect isotopic-$CO_2$ CRDS measurements of $^{13}C$-enriched samples. Resolving this issue is important so that CRDS analysers can be used in $CO_2$ flux studies involving $^{13}C$-labelled tracers.

**METHODS:** We tested a Picarro G2131-i CRDS isotopic-$CO_2$ gas analyser with specialty gravimetric standards of widely varying $^{13}C$ abundance (from natural to 20.1 atom%) and $CO_2$ mole fraction ($xCO_2$: <0.1 to 2116 ppm) in synthetic air. The presence of spectroscopic interference between $^{12}CO_2$ and $^{13}CO_2$ bands was assessed by analysing errors in measurements of the standards. A multi-component calibration strategy was adopted, incorporating isotope ratio and mole fraction data to ensure accuracy and consistency in corrected values of $\delta^{13}C$-$CO_2$, $x^{12}CO_2$, and $x^{13}CO_2$.

**RESULTS:** CRDS measurements of $x^{13}CO_2$ were found to be accurate throughout the tested range (<0.005 to 100 ppm). On the other hand, spectral cross-talk in $x^{12}CO_2$ measurements of standards containing elevated levels of $^{13}CO_2$ led to inaccuracy in $x^{12}CO_2$, total-$xCO_2$ ($x^{12}CO_2$ + $x^{13}CO_2$), and $\delta^{13}C$-$CO_2$ data. An empirical relationship for $x^{12}CO_2$ measures that incorporated $^{13}C/^{12}C$ isotope ratio (i.e. $^{13}CO_2/^{12}CO_2$, $R_{CO_2}$) as a secondary (non-linear) variable was found to compensate for the perturbations, and enabled accurate instrument calibration for all $CO_2$ compositions covered by our standard gases.

**CONCLUSIONS:** $^{13}C$-enrichement in $CO_2$ leads to minor errors in CRDS measurements of $x^{12}CO_2$. We propose an empirical correction for measurements of $^{13}C$-enriched $CO_2$ in air by CRDS instruments such as the Picarro G2131-i.

## Introduction

Cavity ring-down spectroscopy (CRDS) is an advanced laser absorption method[1-3] gaining prominence for measuring trace gases in air. The high sensitivity of CRDS has allowed development of analysers tuned to detect multiple isotopologues,[4-6] meaning that isotope ratios and mole fractions of trace-gases may be concurrently measured. With similar precision[7] to conventional continuous flow isotope-ratio mass spectrometry (IRMS) but at lower measurement cost basis,[8] isotopic CRDS is poised to displace traditional analytical instruments and open new research possibilities.

A frequent application of isotope ratio CRDS is $\delta^{13}C$ measurement of atmospheric $CO_2$.[9] $\delta^{13}C$-$CO_2$ values are widely used in carbon cycling studies,[10-12] paleoclimatology,[13, 14] oceanography,[15] and atmospheric science.[16] Monitoring of greenhouse gas emissions as well as $CO_2$ sequestration and storage integrity are further applications.[17, 18] Although isotopic-$CO_2$ CRDS is principally used for measuring $\delta^{13}C$-$CO_2$ values, the simultaneous acquisition of high resolution $CO_2$ mole fraction data ($xCO_2$) is often helpful, for instance in biomedical metabolic flux analysis[5, 19] and ecosystem soil respiration experiments.[20, 21]

Significant evaluative work has been conducted on isotopic-$CO_2$ CRDS at natural $^{13}C$ abundances.[7, 9, 22-26] Corrective strategies for $H_2O$ interference,[27, 28] background gas-matrix perturbation effects,[23, 29, 30] and concentration dependence[20, 29-32] on $\delta^{13}C$-$CO_2$ measurements are known. The characterisation and elimination of $H_2S$ interference have also been described.[33] However, limited attention has been paid to CRDS analysis of $^{13}C$-enriched samples despite possible cross-talk between $^{12}CO_2$ and $^{13}CO_2$ spectral features at high $^{13}C$ abundances. Assessing instrument performance and potential spectral interference

under such conditions is important if CRDS is to be applied to experiments involving $^{13}C$-labelled tracers, such as those performed for studying the microbial decomposition of organic matter in soil,[34] or in research of plant metabolism.[35] In such cases, in addition to practical advantages,[26, 36] accurate isotopic-$CO_2$ CRDS at high $^{13}C$ abundances would significantly improve empirical precision via reduction of uncertainty in isotopic partitioning of $CO_2$ fluxes.[37]

In this study, we tested isotopic-$CO_2$ CRDS for accuracy and spectral cross-talk over a wide range of $^{13}C$-contents (from natural abundance to 20.1 atom%) and $CO_2$ mole fractions (<0.1 to 2116 ppm). Small but detectable interference from $^{13}CO_2$ on $^{12}CO_2$ measures was observed at high $^{13}C$ abundances. We present a multi-component calibration strategy and empirical correction for compensating affected measurements of $^{12}CO_2$ and, indirectly, $\delta^{13}C$-$CO_2$ values. Our results are important for future refinement of CRDS instrumentation and for researchers employing CRDS analysers to measure $^{13}C$-enriched $CO_2$ in air.

## Methods

### *Cavity ring-down spectrometer*

The instrument used in this study was a G2131-i isotopic-$CO_2$ CRDS gas analyser (Picarro Inc., Santa Clara, CA, USA). The G2131-i measures spectral lines of $^{12}C^{16}O_2$ and $^{13}C^{16}O_2$ in a controlled optical cavity (35 $cm^3$, held at 318.150 ± 0.002 K and 18.67 ± 0.02 kPa). A vacuum pump and automatic valve system continuously circulate sample gas through the cavity with an inlet flow rate of ca 25 mL $min^{-1}$ (NTP), while measurement data are returned at a rate of ca 0.8 Hz. The spectral features measured are the R(36) 30013←00001 band

centred at 6251.760 $cm^{-1}$ for $^{12}C^{16}O_2$, and the R(12) 30012←00001 transition of $^{13}C^{16}O_2$ at 6251.315 $cm^{-1}$ (Figure 1). The analyser repeatedly assesses ring-down times across each feature to construct optical absorption spectra. Galatry[38] spectral models are automatically fitted to the spectra,[39, 40] and modelled absorption peak heights used for calculating mole fractions of $^{12}C^{16}O_2$ and $^{13}C^{16}O_2$, while $\delta^{13}C$-$CO_2$ values are determined from the ratio of the $^{13}C^{16}O_2$ and $^{12}C^{16}O_2$ peak heights.[41]

However, spectral interferences from $CH_4$ and $H_2O$ complicate the $CO_2$ measurements. To mitigate these, the G2131-i also measures spectral lines of $^{12}C^{1}H_4$ and $^{1}H_2{}^{16}O$ (respectively centred at 6056.84 and 6057.80 $cm^{-1}$; not shown), which are used to correct raw $CO_2$ peak measurements. The $H_2O$ corrections are comprehensively described elsewhere,[27, 28, 41] while compensation of $CH_4$ interference[9] is explained in notes[41, 42] from the instrument manufacturer (see also supporting material 1: Table S2).

After the $CH_4$ and $H_2O$ corrections, the G2131-i applies separate linear calibration transformations (i.e. Beer-Lambert law, see supporting material 1: Table S3) to the corrected spectral peak data of $^{12}C^{16}O_2$, $^{13}C^{16}O_2$, and their ratio (i.e. $^{13}C^{16}O_2/^{12}C^{16}O_2$ to independently give $\delta^{13}C$-$CO_2$).[41] This approach is problematic as it invites systematic disagreement in output results – because fixing any two values of $x^{12}CO_2$, $x^{13}CO_2$, and $\delta^{13}C$-$CO_2$ automatically determines the third, individual calibrations for all three leads to contradictory, overdetermined data. Although such inconsistency may be overlooked in certain contexts (if accurate $xCO_2$ data are not required for example), in our view, the possibility for artificial error represents an oversight in G2131-i calculation logic. We describe an alternative approach that ensures consistency in final $CO_2$ values (see below).

*Potential for spectral cross-talk between $^{12}CO_2$ and $^{13}CO_2$*

Apart from $H_2O$ and $CH_4$, no other interferences to $CO_2$ absorptions are considered by the G2131-i system. Examining the spectral region,[43, 44] however (Figure 1), a potential source of additional interference is the R(10) 31112←01101 $^{13}C^{16}O_2$ transition at 6251.716 $cm^{-1}$ that shoulders the R(36) $^{12}C^{16}O_2$ feature (measured by the G2131-i from 6251.65 to 6251.86 $cm^{-1}$). At natural abundance $^{13}C$ the comparative magnitude of these two absorptions differs by a factor of more than 700, making any interference negligible. However, in our focus on $^{13}C$-enriched $CO_2$, this presumption may not hold, and measurement error in $^{12}C^{16}O_2$ may result. For instance, at 10 atom% $^{13}C$ the R(36) $^{12}C^{16}O_2$ absorption is only 70 times greater than the R(10) $^{13}C^{16}O_2$ band. While such potential perturbation may seem minor, work by Malowany et al[33] concerning $H_2S$ interference on $CO_2$ spectroscopy shows that even a small shouldering overlap from unanticipated transitions can result in disruption to $^{12}C^{16}O_2$ and $^{13}C^{16}O_2$ measurements (and subsequently to $\delta^{13}C$-$CO_2$ values). The potential for interference is visualised most sharply in the total absorption spectrum for equimolar fractions of $^{12}CO_2$ and $^{13}CO_2$ in air (i.e. 50 atom% $^{13}C$; Figure 1 inset).

In contrast to the R(36) $^{12}C^{16}O_2$ transition, no unaddressed cross-talk interferences are likely to affect the R(12) $^{13}C^{16}O_2$ measurement band (6251.21 to 6251.40 $cm^{-1}$, Figure 1). The only possible conflict is the $^{12}C^{16}O^{17}O$ absorption at 6151.383 $cm^{-1}$, but this is ca 1200 times smaller than the $^{13}C^{16}O_2$ feature at natural abundance $^{17}O$. (For completeness we also mention that the $^{12}C^{16}O^{18}O$ spectral bands at 6251.611 and 6251.785 $cm^{-1}$ have respective absorptions 650 and 6000 times less than the R[36] $^{12}C^{16}O_2$ transition at natural abundance $^{18}O$, meaning that neither are plausible sources of interference in samples containing natural distributions of oxygen isotopes.)

*Standard gases: preparation and composition*

To investigate possible cross-talk between $CO_2$ species and any effect on G2131-i performance, five high-precision $^{13}C$-enriched gravimetric standard gas mixtures were prepared by Linde Gas Benelux B.V. (Dieren, The Netherlands). The standard mixtures were composed of $^{13}C$-enriched and natural abundance $CO_2$ sources (Sigma-Alrich Corp., St. Louis, MO, USA), and were balanced with high purity $O_2$ and $N_2$. Standards were designed to conform to G2131-i performance specifications, with total-$x$$CO_2$ (i.e. $x^{12}CO_2 + x^{13}CO_2$) ranging from 429 ppm to 2116 ppm. Meanwhile the $^{13}C$-content varied from near natural abundance to 20.1 atom% (i.e. $\delta^{13}C$-$CO_2$ values from ca -36 ‰ to +21500 ‰ vs VPDB[45]). In addition to $^{13}C$-enriched standards, two natural $^{13}C$ abundance standard airs and a standard zero air were also sourced (Praxair N.V., Oevel, Belgium; Air Liquide S.A., Paris, France). All standards were prepared moisture-free;[46] composition data are presented in Table 1. Uncertainties on $^{13}C$-enriched standards were calculated using error propagation methods[47] incorporating gravimetric, isotopic, and molar mass precisions inherent to the preparation process (sensitivity of the gravimetric balance and isotopic purity of the $^{13}C$-enriched $CO_2$ source were the largest contributors of uncertainty). These resulting uncertainties (Table 1) effectively placed tolerance limits on the standard values – limits within which accurate CRDS measurements should lie (complete calculations set out in supporting material 2). The natural $^{13}C$ abundance standard airs had certified levels of total-$x$$CO_2$ (from which the CRDS relevant $x$$C^{16}O_2$ values were deduced, Table 1) while their $\delta^{13}C$-$CO_2$ values were determined using a trace-gas preparation unit (ANCA-TGII, Sercon Ltd, Crewe, UK) interfaced to a SerCon 20-20 isotope ratio mass spectrometer. The IRMS measurements were calibrated with VPDB reference standards and carried an uncertainty of 0.3 ‰.

One complication of the $^{13}C$-enriched standards was the presence of $^{18}O$-enriched $CO_2$, which was introduced from the initial $^{13}C$-enriched $CO_2$ source (99 atom% $^{13}C$, 2.0 atom% $^{18}O$). Although $CO_2$ species containing $^{18}O$ (and $^{17}O$) are not detected by the G2131-i, there is potential for interference from any significant increase in $^{12}C^{16}O^{18}O$ (see above). Fortunately, because only small amounts of the $^{13}C$-enriched $CO_2$ source were used in producing the standard mixtures, we determined that the $\delta^{18}O$-$^{12}CO_2$ values in the final standards were no more than ca +50 ‰ vs VSMOW[45]. Consequently, interference from $^{12}C^{16}O^{18}O$ was not a concern and we could reasonably disregard the excess $^{18}O$. For clarity, we report $^{12}C^{16}O_2$ and $^{13}C^{16}O_2$ isotopologue data (Table 1) and use these in all calibration calculations before separately applying a final oxygen isotope scaling-factor to align calibrated $^{12}C^{16}O_2$ and $^{13}C^{16}O_2$ measurements to their would-be $^{12}CO_2$ and $^{13}CO_2$ mole fractions at natural abundances of oxygen isotopes.

*Standard gases: gas-matrix pressure broadening corrections*

Since our $^{13}C$-enriched standards were balanced with $N_2$ and $O_2$ but not Ar, the $CO_2$ spectroscopy differed slightly from that of ambient air due to gas-matrix pressure broadening effects (PBEs). To ameliorate these distortions, we applied adjustments to the gravimetric values of the prepared standards to give apparent $CO_2$ mole fractions and $^{13}C/^{12}C$ isotope ratios that an accurately calibrated G2131-i instrument should report (i.e. $CO_2$ composition equivalents, as though the standards had been balanced by $CO_2$-free ambient air).

Significant work has been conducted on the PBEs of $CO_2$ spectral absorptions relevant to the G2131-i,[48-56] with the empirical effects of different buffer-gas compositions on CRDS comprehensively documented.[29, 30, 57-59] We assessed the correction method of Friedrichs et

al[29] as suitable for making PBE adjustments in our work, and preliminary testing of the G2131-i indicated performance consistent with their findings. Briefly, Friedrichs et al apply a single line shape correction for PBEs on $CO_2$ mole fraction data and use a separate $\delta^{13}C$ offset factor to adjust for divergence between R(36) $^{12}C^{16}O_2$ and R(12) $^{13}C^{16}O_2$ bands (and thus $\delta^{13}C$-$CO_2$ measurements). We found excellent agreement between the empirical correction of Friedrichs et al and the relative buffer-gas pressure broadening coefficients of the R(36) $^{12}C^{16}O_2$ transition as described in specialist studies.[50-54, 59-61] On the other hand, we were unable to find any literature on pressure broadening coefficients for the R(12) $^{13}C^{16}O_2$ transition in order to compare the $\delta^{13}C$ offsets, although we note that the spectroscopic simulations of Friedrichs et al are in close agreement with their empirical findings.

While Friedrichs et al[29] do not provide uncertainty analysis in their correction scheme, Nara et al[58] report standard errors for their PBE measurements of the R(12) 30013←00001 $^{12}C^{16}O_2$ transition in a sister CRDS instrument (Picarro G2301). Applying the errors observed by Nara et al to our calculations yielded ca 4.5 % relative uncertainties on the PBEs in $^{12}C^{16}O_2$. To remove all doubt, we therefore incorporated 9 % uncertainties on our PBE adjustments. We similarly incorporated uncertainties on the $^{13}C^{16}O_2$ corrections derived from Friedrichs et al by placing conservative margins on their $\delta^{13}C$ offset factors. $CO_2$ self-broadening effects were omitted as negligible (which, if detectable, would be seen as non-linearity in the CRDS absorption-abundance response). Finalised PBE corrections and apparent $CO_2$ compositions that an accurate G2131-i should measure for the $^{13}C$-enriched standards are presented in Table 1 (for details see supporting material 2).

*Measurements of standard gases*

Standards were measured in an environmentally controlled laboratory (20 °C) to ensure stable conditions for analyser operation. Measurements were conducted by connecting gas bottles to the G213i-i inlet port via a regulated union (10 kPa gauge pressure). Each standard was pumped through the optical cavity for more than one hour before recording any formal data. This prolonged 'flush period' of each standard ensured that all transient memory effects due to dilution, contamination, and surface sorption were eliminated. Once readings stabilised, 10-minutes of data (ca 460 data points) were recorded and averaged. Standard deviations of the aggregate data were calculated to provide measurement uncertainties. In addition to the instrument reported $CO_2$ data, raw spectral peak absorption values were reconstructed (see supporting material 1 and 3) to serve as principal measures for assessing the G2131-i, thereby circumventing any ambiguity created by inconsistencies in the internal calculations (see above). All the measurement and reconstructed data are collated in supporting material 3.

*Calibration strategy*

Conventional calibration of isotope ratio data involves adjustment of sample measures against standards of known or assumed isotopic values. Corrections are generally accomplished by 1-point offsets or 2-point interpolations, and standards are chosen that are as close as possible to unknown sample values.[31] The principal errors that calibrations of $\delta^{13}C$-$CO_2$ measures usually address are concentration dependence and instrument drift;[22] unknown sample values are adjusted precisely, and final uncertainties typically derive from measurement precision rather than from uncertainties on standards.[9]

In the present study, we faced a different set of considerations. (i) Multiple standards with inexactly known compositions would not be utilised effectively by usual interpolation calibrations. (ii) The standards were also intended to test for cross-talk in G2131-i spectral measurements. (iii) We aimed to deploy a single calibration model that would deliver accuracy in both mole fraction and isotope ratio data across a broad range of $^{13}C$ abundances and $xCO_2$ levels.

As a first appraisal, we compared G2131-i reported $CO_2$ data (i.e. measurements as per the factory calibration) with PBE adjusted gravimetric standard data (Figure 2). While the factory calibration of our G2131-i was accurate to the uncertainty tolerances of all standards in $\delta^{13}C$-$CO_2$ values (shown as $R_{CO_2}$, Figure 2c), there were significant residual errors in the $x^{12}C^{16}O_2$ data (Figure 2b), and the $x^{13}C^{16}O_2$ data were entirely inaccurate (Figure 2a).

To improve overall accuracy and data coherence, we implemented an alternative approach whereby calibrations were applied only to $x^{12}C^{16}O_2$ and $x^{13}C^{16}O_2$ measurements, with $\delta^{13}C$-$CO_2$ and total-$xC^{16}O_2$ values being subsequently calculated from corrected measures. However, rather than performing independent calibrations, $x^{12}C^{16}O_2$ and $x^{13}C^{16}O_2$ were jointly corrected through an enlarged optimisation problem (a multi-component calibration) that incorporated all available data from the gravimetric standards and also accounted for varying uncertainties on standard values.

For the case of linear relationships between spectral peak heights and $CO_2$ isotopologue mole fractions, the primary calibration equations were as follows:

$$x^{12}\mathrm{C}^{16}\mathrm{O}_2 = (12_{rep} + A_{12}) \cdot B_{12} \,/\, wd\_ratio \qquad (1)$$

$$x^{13}C^{16}O_2 = (13_{rep} + A_{13}) \cdot B_{13} \,/\, wd\_ratio \quad (2)$$

where $12_{rep}$ and $13_{rep}$ are the respective $CH_4$-$H_2O$-corrected spectral absorption peak heights reported for $^{12}C^{16}O_2$ and $^{13}C^{16}O_2$ (respectively termed *peak87_baseave_spec* and *peak88_baseave_spec* in the G2131-i data system, see supporting material 1), $A_{12}$-$B_{13}$ are empirical coefficients, and *wd_ratio* is an ancillary $H_2O$ correction variable used by the G2131-i for adjusting $x$CO$_2$ data to a dry mole fraction basis (i.e. the variable compensates for molar dilution caused by any water vapour present in samples; see supporting material 1 Table S2, and also Rella[27] and Hoffnagle[41] – if $H_2O$ mole fraction = 0 then *wd_ratio* = 1). From these calibrated data, total-$x$C$^{16}$O$_2$, the $^{13}C/^{12}C$ isotope ratio ($R_{CO_2}$), and $\delta^{13}$C-CO$_2$ values were calculated:

$$xC^{16}O_2 = x^{12}C^{16}O_2 + x^{13}C^{16}O_2 \quad (3)$$

$$R_{CO_2} = \frac{x^{13}C^{16}O_2}{x^{12}C^{16}O_2} \quad (4)$$

$$\delta^{13}C\text{–}CO_2 = \left[\left(\frac{R_{CO_2}}{R_{VPDB}}\right) - 1\right] \cdot 1000\ ‰ \quad (5)$$

Calibration coefficients ($A_{12}$, $B_{12}$, $A_{13}$, and $B_{13}$) were found through weighted least squares (WLS) optimisation of Eqs. (1)-(4), with G2131-i measurements used as input data ($12_{rep}$, $13_{rep}$, *wd_ratio*; supporting material 3) and PBE adjusted standard values (Table 1) substituting the dependent variables in each equation (i.e. reverse regression). Residual weights were taken as the reciprocals of the summed variances resulting from the uncertainty

on the relevant standard and the raw measurement's standard deviation. This procedure was similar to the weighted total least squares analysis (cf. orthogonal regression) described by Krystek and Anton[62] and used by Stowasser et al[39] for CRDS calibration (we could not fully adopt that method as it only applies to simple linear regression). The weightings allowed diverse data (i.e. mole fraction and isotope ratio) to be proportionally included into a single analysis, and meant that a least squares solution would, on aggregate, calibrate the measurements to within the uncertainties of each standard value (we considered a calibration model to be 'accurate' if all calibrated measures were within their respective uncertainty limits, e.g. Figure 2a). The WLS solution was found with R (version 3.2.1)[63] using general purpose optimisation with the L-BFGS-B algorithm[64] to yield the best-fit calibration for all available standard data (n = 31).

By examining residual errors in linear calibration, we assessed the presence of spectral cross-talk between $^{12}CO_2$ and $^{13}CO_2$. Expecting an interference from the R(10) $^{13}C^{16}O_2$ transition on $^{12}C^{16}O_2$ measurements (see above, Figure 1), we postulated a generic relationship between the 'true' optical absorption peak height of the R(36) $^{12}C^{16}O_2$ transition ($12_{true}$) and the interference-affected G2131-i reported measurement ($12_{rep}$):

$$12_{rep} = 12_{true} \cdot [1 + f(z)] + g(z) \qquad (6)$$

where $f(z)$, $g(z)$ are hypothetical functions of an unknown secondary variable $z$ that characterises spectral distortion on the $^{12}CO_2$ measurement. With a suitable variable and function(s), Eq. (6) may be used to modify Eq. (1) and provide an interference correcting calibration for $x^{12}C^{16}O_2$, which may then be optimised in the same manner as described for a simple linear model.

## Results and discussion

### *Linear calibration*

WLS optimisation of the multi-component linear calibration model (Eqs. 1–4) yielded a similar outcome to the factory configuration (Figure 3; coefficients in Table 2) except that the resulting $x^{12}C^{16}O_2$, $x^{13}C^{16}O_2$, and $\delta^{13}C\text{-}CO_2$ measurement data were internally self-consistent. Consequently, the calibrated $x^{13}C^{16}O_2$ values were accurate throughout the tested composition range (<0.005 to 100 ppm $x^{13}C^{16}O_2$) with all residuals falling within the uncertainty tolerances and no limit-of-linearity reached (Figure 3a). This is an important demonstration of G2131-i performance outside its specified operating envelope. On the other hand, as with the factory-set calibration, a linear model was not accurate for $x^{12}C^{16}O_2$ measurements, with several residual errors significantly larger than the aggregate uncertainties on standard compositions (Figure 3b). These small inaccuracies also gave rise to incorrect $R_{CO_2}$ (Figure 3c) and total-$xC^{16}O_2$ data (not shown). To achieve accurate calibration, a different functional form was thus required for $^{12}CO_2$ measurements.

### *Non-linear calibration model*

Under a linear response model of optical absorption and molecular abundance, G2131-i measures for $x^{12}C^{16}O_2$ were progressively reduced (under-measured) at higher levels of $^{13}CO_2$ (Figure 3b). This was contrary to our expectation that spectral overlap would lead to overestimation in absorption peak height. We speculate that the origin of this phenomenon is a fitting artefact caused by imposing a single peak spectral model to ring-down measurements of the $^{12}C^{16}O_2$ spectral feature (a similar phenomenon is observed[33] from $H_2S$ interference

on $^{13}CO_2$). If our supposition is correct, because the R(10) $^{13}C^{16}O_2$ transition lies at a shouldering wavenumber, it partly disrupts the baseline of the larger R(36) $^{12}C^{16}O_2$ transition (e.g. Figure 1 inset). As a result, fitting a single peak spectral model to the overlapped spectrum raises the baseline and decreases the reported peak height. We were able to reproduce this outcome by testing Voigt and Galatry peak-fitting algorithms with constant half-width parameters on simulated[44] spectra. However, observed measurement perturbations could not be characterised theoretically as details of the spectroscopic model used in the G2131-i are not publicly available.

Notwithstanding the lack of a precise spectroscopic correction or revision, we devised an empirical model approximating the observed deviations. Following our inference that $x^{12}C^{16}O_2$ errors were caused by the R(10) $^{13}C^{16}O_2$ absorption, residuals of the linear calibration were examined against $^{13}C^{16}O_2$ mole fraction (Figure 4a). While a negative correlation was observed, considerable remaining variance indicated that the interference is more complex than a linear adjustment. This is unsurprising given that a baseline aberration is probably a function of the relative size of the interfering absorption as opposed to its absolute magnitude. Accordingly, comparing $x^{12}C^{16}O_2$ residuals with standard $R_{CO_2}$ values revealed a definite, albeit non-linear, relationship to the measurement errors (Figure 4b). Trialling numerous potential corrective formulae (smooth continuous functions with no more than two parameters plus an intercept and no local inflections throughout the assessed $CO_2$ range), we found that an exponential relation of $R_{CO_2}$ would fit the residual errors (dashed line, Figure 4b). We therefore developed an appropriate form for Eq. (6) using $R_{CO_2}$ as variable $z$:

$$12_{rep} = 12_{true} \cdot \left[1 + \mathrm{C} \cdot e^{\mathrm{D} \cdot R\mathrm{co}_2}\right] \quad (7)$$

where C and D are constant terms. Using Eq. (7) to amend Eq. (1), and substituting $x^{13}C^{16}O_2/12_{rep}$ as a proxy for $R_{CO_2}$, an improved calibration equation for $x^{12}C^{16}O_2$ was found:

$$x^{12}C^{16}O_2 = \frac{(12_{rep} + A_{12}) \cdot B_{12}}{\left[1 + C_{12} \cdot e^{D_{12} \cdot \left(\frac{x^{13}C^{16}O_2}{12_{rep} + A_{12}}\right)}\right]} / wd\_ratio \quad (8)$$

with $C_{12}$ and $D_{12}$ as additional coefficients that characterise the interference correction term and $x^{13}C^{16}O_2$ being determined from Eq. (2). WLS optimisation of Eq. (8) together with Eqs. (2)-(4) resulted in a calibration model (Table 2) where all measurement data (i.e. $x^{12}C^{16}O_2$, $x^{13}C^{16}O_2$, $R_{CO_2}$, and total-$xC^{16}O_2$) were within the uncertainties on the gravimetric values (Figure 5, and supporting material 3).

*Evaluation and application*

Despite $^{13}CO_2$ interference, linear calibration of G2131-i $x^{12}C^{16}O_2$ measurements achieved reasonable accuracy in all the $^{13}$C-enriched standards that we tested (all relative residual errors ≤0.67 %, averaging 0.32 %). However, these residual errors were larger than the resolution afforded by the G2131-i and uncertainties on gravimetric standards. In compensating for the measures with a non-linear function of $R_{CO_2}$, our revised calibration model ensured that all the corrected $x^{12}C^{16}O_2$ values were within the combined uncertainty limits of $^{13}$C-enriched standards (i.e. ≤0.15 %), and had a mean relative residual error of 0.04 % (i.e. an 8-fold improvement on the linear model).

In contrast, linear calibration of $x^{13}C^{16}O_2$ was accurate for all standards tested (irrespective of which $^{12}CO_2$ model – Eq. 1 or 8 – was used for optimisation), although the comparatively

larger gravimetric uncertainties may have obscured small interferences or non-linearity. The relative residual errors in the calibrated $x^{13}C^{16}O_2$ data averaged 0.40 % while the largest corresponding uncertainty on the $^{13}C$-enriched gravimetric standards was 0.71 %.

In terms of complete calibration efficacy, we reiterate that errors in $x^{12}C^{16}O_2$ data (when using linear calibration) also caused inaccuracy in $R_{CO_2}$ and total-$xC^{16}O_2$ (Figure 3, and supporting material 3). However, with the $^{13}CO_2$ correction applied, the calibrated $R_{CO_2}$ and total-$xC^{16}O_2$ data were accurate to the determined uncertainty limits on the gravimetric standards (respective mean relative residuals errors of 0.37 % and 0.03 % while the largest uncertainty on the standards was 0.81 % for $R_{CO_2}$ and 0.11% for total-$xC^{16}O_2$; see Table 1, and supporting material 2 and 3). All measurements of natural abundance $CO_2$ standard airs were also accurate under the $^{13}CO_2$ correction of $x^{12}C^{16}O_2$. In comparison with conventional calibrations of CRDS isotope ratio measurements,[22, 31] our approach precluded the typical issue of concentration dependence (accurate calibration in $x^{12}C^{16}O_2$ and $x^{13}C^{16}O_2$ eliminated the need for direct correction of $\delta^{13}C$-$CO_2$ values). In summary, our non-linear calibration was accurate with every gravimetric standard that we tested. Overall, the weighted residual square errors for the complete linear calibration model totalled 110.81, while applying the non-linear correction on $x^{12}C^{16}O_2$ reduced these to 8.82, thus giving our revised calibration a coefficient of partial determination (partial $r^2$) of 0.92 against the linear approach (Table 2).

To apply our calibration strategy to raw G2131-i measurement data (using either our non-linear model or a normal linear equation for $^{12}CO_2$), a post-correction workbook is supplied (supporting material 4). While calibration constants may vary temporally and between individual G2131-i analysers, given the minimal drift and inter-instrument consistency observed in other studies,[9, 22, 65] we expect that reasonable accuracy may be achieved by

cautious application of our correction model to measurements of $^{13}C$-enriched $CO_2$ samples by other G2131-i units. In any case, the results and methods reported here are a template for G2131-i users and may be extended to other laser absorption instruments sharing the same $CO_2$ spectroscopy (e.g. Picarro G2201-i).

Although our multi-component calibration improves upon conventional methods used for CRDS, we note that it is only relevant for measurements where both high accuracy $CO_2$ mole fraction and $\delta^{13}C$-$CO_2$ data are simultaneously required. G2131-i users unconcerned with small errors in $xCO_2$ and $\delta^{13}C$-$CO_2$ at high $^{13}C$ abundances will achieve acceptable accuracy using simple linear calibration models. Furthermore, our non-linear correction to $^{12}CO_2$ measurements is unnecessary where G2131-i measurements cover only a narrow band of $\delta^{13}C$-$CO_2$ values (e.g. natural abundance samples). This is because the correction term remains proportionally constant for a given value of $R_{CO_2}$ irrespective of $CO_2$ mole fraction (Eq. 7), and so linear calibration will be accurate when the $^{13}C/^{12}C$ isotope ratios of unknown samples and calibration standards are similar.

In addition, while the $^{12}CO_2$ correction presented in this work fits all the tested gravimetric standard data, the associated uncertainties mean that other mathematical functions (e.g. power, polynomial) could equally account for the observed measurements. A more extensive investigation of G2131-i measurements at elevated levels of $^{13}CO_2$ is required to verify if our negative exponential equation of $R_{CO_2}$ (Eq. 7) accurately represents $^{13}CO_2$ interference on the R(36) $^{12}C^{16}O_2$ transition, and hence determine whether a different correction function is more suitable (particularly for $CO_2$ compositions outside the range that we measured). We expect that careful gas blending experiments employing dynamic mass flow control mixers such as those used by Rella et al[28], Nara et al[58] and Friedrichs et al[29] will enable a more exact

quantification of $x^{12}C^{16}O_2$ measurement errors. From our calibration model we may derive the expected distortion that $^{13}CO_2$ addition causes on G2131-i measurements of $^{12}CO_2$ (Fig. 6) – a prediction that may be expressly tested by such blending experiments.

**Conclusions**

CRDS is an increasingly popular and versatile method for the isotopic analysis of atmospheric trace-gases. However, due to narrow separation between spectroscopic bands of different isotopologues, there is potential for cross-talk interferences in CRDS measurements. While not an issue for samples with natural abundance $^{13}C$, we found errors in the Picarro G2131-i isotopic-$CO_2$ analyses of gravimetric standard gases highly enriched in $^{13}C$. Evidenced as under-measurement in $x^{12}C^{16}O_2$ (and therefore overestimation of $\delta^{13}C$-$CO_2$ values), the observed errors were putatively caused by interference from a secondary $^{13}C^{16}O_2$ transition shouldering the primary $^{12}C^{16}O_2$ absorption. We suspect that spectroscopic overlap distorts the baseline fitting of the spectral model used in the G2131-i, leading to under-estimation of $x^{12}C^{16}O_2$ at elevated levels of $^{13}CO_2$ (conversely, $x^{13}C^{16}O_2$ data were not affected). If our conjecture is correct, redressing the principal source of $x^{12}CO_2$ error in G2131-i measurements should be possible by implementing a new spectral model in instrument software or by shifting the spectroscopy to an unimpeded $^{12}C^{16}O_2$ transition.

In lieu of resolving the direct cause of the inaccuracies, a non-linear correction can be applied to $x^{12}C^{16}O_2$ measurements. By using a multi-component calibration strategy where mole fraction and isotope ratios are jointly optimised against standards, G2131-i measurements can be adjusted to provide accurate data across a wide range of $CO_2$ compositions. Researchers can directly implement or adapt our correction scheme using materials supplied in the

supporting material. While our calibration model requires further validation, it nevertheless improves the measurement accuracy of $^{13}C$-enriched $CO_2$ samples compared with a conventional approach. In addition to the G2131-i analyser, these methods may be employed with other isotopic-$CO_2$ instruments that share the same spectroscopic architecture.

**Acknowledgements**

We acknowledge Lex van Leeuwen and Linde Gas Benelux B.V. for their service and cooperation in producing $^{13}C$-enriched specialty gravimetric standard gases. We are grateful to our colleagues Stijn Vandevoorde and Katja Van Nieuland for their assistance. Renato Winkler and Nabil Saad from Picarro Inc. provided useful information and advice concerning the spectroscopy of the G2131-i analyser. Finally, we thank three anonymous reviewers whose comments helped improve this paper.

**Supporting information**

1. Details of G2131-i datalog and measurement calculations
2. Gravimetric standard calculations, uncertainties, and PBE calculations
3. Raw measurement data, reconstructed data, linear calibrated data, non-linear calibrated data
4. Data post-correction workbook

## References


[1] A. O'Keefe, D. A. G. Deacon. Cavity ring-down optical spectrometer for absorption measurements using pulsed laser sources. *Rev. Sci. Instrum.* **1988**, *59*, 2544.

[2] R. T. Jongma, M. G. H. Boogaarts, I. Holleman, G. Meijer. Trace gas detection with cavity ring down spectroscopy. *Rev. Sci. Instrum.* **1995**, *66*, 2821.

[3] M. D. Wheeler, S. M. Newman, A. J. Orr-Ewing, M. N. R. Ashfold. Cavity ring-down spectroscopy. *J. Chem. Soc., Faraday Trans.* **1998**, *94*, 337.

[4] H. Dahnke, D. Kleine, W. Urban, P. Hering, M. Mürtz. Isotopic ratio measurement of methane in ambient air using mid-infrared cavity leak-out spectroscopy. *Appl. Phys. B* **2001**, *72*, 121.

[5] E. R. Crosson, K. N. Ricci, B. A. Richman, F. C. Chilese, T. G. Owano, R. A. Provencal, M. W. Todd, J. Glasser, A. A. Kachanov, B. A. Paldus, T. G. Spence, R. N. Zare. Stable isotope ratios using cavity ring-down spectroscopy: Determination of $^{13}C/^{12}C$ for carbon dioxide in human breath. *Anal. Chem.* **2002**, *74*, 2003.

[6] E. R. T. Kerstel, R. Q. Iannone, M. Chenevier, S. Kassi, H. J. Jost, D. Romanini. A water isotope ($^{2}H$, $^{17}O$, and $^{18}O$) spectrometer based on optical feedback cavity-enhanced absorption for in situ airborne applications. *Appl. Phys. B* **2006**, *85*, 397.

[7] E. M. Berryman, J. D. Marshall, T. Rahn, S. P. Cook, M. Litvak. Adaptation of continuous-flow cavity ring-down spectroscopy for batch analysis of $\delta^{13}C$ of $CO_2$ and comparison with isotope ratio mass spectrometry. *Rapid Commun. Mass Spectrom.* **2011**, *25*, 2355.

[8] Picarro. *WS-CRDS for Isotopes – Cost of Measurement Comparison with IRMS for Liquid Water*, Picarro Inc., Sunnyvale, California, USA, **2009**.

[9] F. R. Vogel, L. Huang, D. Ernst, L. Giroux, S. Racki, D. E. J. Worthy. Evaluation of a cavity ring-down spectrometer for in situ observations of $^{13}CO_2$. *Atmos. Meas. Tech.* **2013**, *6*, 301.

[10] M. S. Torn, S. C. Biraud, C. J. Still, W. J. Riley, J. A. Berry. Seasonal and interannual variability in $^{13}C$ composition of ecosystem carbon fluxes in the US Southern Great Plains. *Tellus B* **2011**, *63*, 181.

[11] D. Yakir, L. d. S. L. Sternberg. The use of stable isotopes to study ecosystem gas exchange. *Oecologia* **2000**, *123*, 297.

[12] W. Mook. $^{13}C$ in atmospheric $CO_2$. *Neth. J. Sea Res.* **1986**, *20*, 211.

[13] R. J. Francey, C. E. Allison, D. M. Etheridge, C. M. Trudinger, I. G. Enting, M. Leuenberger, R. L. Langenfelds, E. Michel, L. P. Steele. A 1000-year high precision record of $\delta^{13}C$ in atmospheric $CO_2$. *Tellus B* **2011**, *51*, 170-191.

[14] T. K. Bauska, D. Baggenstos, E. J. Brook, A. C. Mix, S. A. Marcott, V. V. Petrenko, H. Schaefer, J. P. Severinghaus, J. E. Lee. Carbon isotopes characterize rapid changes in atmospheric carbon dioxide during the last deglaciation. *Proc. Natl. Acad. Sci. USA* **2016**, *113*, 3465.

[15] A. Mix, N. Pisias, R. Zahn, W. Rugh, C. Lopez, K. Nelson. Carbon 13 in Pacific Deep and Intermediate Waters, 0-370 ka: Implications for Ocean Circulation and Pleistocene $CO_2$. *Paleoceanography* **1991**, *6*, 205.

[16] S. S. Assonov, C. A. M. Brenninkmeijer, T. J. Schuck, P. Taylor. Analysis of $^{13}C$ and $^{18}O$ isotope data of $CO_2$ in CARIBIC aircraft samples as tracers of upper troposphere/lower stratosphere mixing and the global carbon cycle. *Atmos. Chem. Phys.* **2010**, *10*, 8575.

[17] B. Galfond, D. Riemer, P. Swart. Analysis of signal-to-noise ratio of $\delta^{13}C$-$CO_2$ measurements at carbon capture, utilization and storage injection sites. *Int. J. Greenhouse Gas Control* **2015**, *42*, 307.

[18] S. Krevor, J.-C. Perrin, A. Esposito, C. Rella, S. Benson. Rapid detection and characterization of surface $CO_2$ leakage through the real-time measurement of $\delta^{13}C$ signatures in $CO_2$ flux from the ground. *Int. J. Greenhouse Gas Control* **2010**, *4*, 811.

[19] T. H. Yang, E. Heinzle, C. Wittmann. Theoretical aspects of $^{13}C$ metabolic flux analysis with sole quantification of carbon dioxide labeling. *Comput. Biol. Chem.* **2005**, *29*, 121.

[20] H. S. K. Snell, D. Robinson, A. J. Midwood. Minimising methodological biases to improve the accuracy of partitioning soil respiration using natural abundance $^{13}C$. *Rapid Commun. Mass Spectrom.* **2014**, *28*, 2341.

[21] F. Albanito, J. L. McAllister, A. Cescatti, P. Smith, D. Robinson. Dual-chamber measurements of $\delta^{13}C$ of soil-respired $CO_2$ partitioned using a field-based three end-member model. *Soil Biol. Biochem.* **2012**, *47*, 106.

[22] J. Pang, X. Wen, X. Sun, K. Huang. Intercomparison of two cavity ring-down spectroscopy analyzers for atmospheric $^{13}CO_2/^{12}CO_2$ measurement. *Atmos. Meas. Tech.* **2016**, *9*, 3879.

[23] M. Becker, N. Andersen, B. Fiedler, P. Fietzek, A. Körtzinger, T. Steinhoff, G. Friedrichs. Using cavity ringdown spectroscopy for continuous monitoring of $\delta^{13}C(CO_2)$ and $fCO_2$ in the surface ocean. *Limnol. Oceanogr. Methods* **2012**, *10*, 752.

[24] S. Eyer, B. Tuzson, M. E. Popa, C. van der Veen, T. Röckmann, M. Rothe, W. A. Brand, R. Fisher, D. Lowry, E. G. Nisbet, M. S. Brennwald, E. Harris, C. Zellweger, L. Emmenegger, H. Fischer, J. Mohn. Real-time analysis of $\delta^{13}C$- and $\delta D$-$CH_4$ in ambient air with laser spectroscopy: method development and first intercomparison results. *Atmos. Meas. Tech.* **2016**, *9*, 263.

[25] C. Rella. *Reduced drift, high accuracy stable carbon isotope ratio measurements using a reference gas with the Picarro $\delta^{13}CO_2$ G2101-i gas analyzer*, Picarro Inc., Sunnyvale, California, USA, **2010**.

[26] E. H. Wahl, B. Fidric, C. W. Rella, S. Koulikov, B. Kharlamov, S. Tan, A. A. Kachanov, B. A. Richman, E. R. Crosson, B. A. Paldus, S. Kalaskar, D. R. Bowling. Applications of cavity ring-down spectroscopy to high precision isotope ratio measurement of $^{13}C/^{12}C$ in carbon dioxide. *Isotopes Environ. Health Stud.* **2006**, *42*, 21.

[27] C. Rella. *Accurate stable carbon isotope ratio measurements in humid gas streams using the Picarro $\delta^{13}CO_2$ G2101-i gas analyzer*, Picarro Inc., Sunnyvale, California, USA, **2010**.

[28] C. W. Rella, H. Chen, A. E. Andrews, A. Filges, C. Gerbig, J. Hatakka, A. Karion, N. L. Miles, S. J. Richardson, M. Steinbacher, C. Sweeney, B. Wastine, C. Zellweger. High accuracy measurements of dry mole fractions of carbon dioxide and methane in humid air. *Atmos. Meas. Tech.* **2013**, *6*, 837.

[29] G. Friedrichs, J. Bock, F. Temps, P. Fietzek, A. Körtzinger, D. W. R. Wallace. Toward continuous monitoring of seawater $^{13}CO_2/^{12}CO_2$ isotope ratio and $pCO_2$:

Performance of cavity ringdown spectroscopy and gas matrix effects. *Limnol. Oceanogr. Methods* **2010**, *8*, 539.

[30] L. A. Konopel'ko, V. V. Beloborodov, D. V. Rumyantsev, Y. K. Chubchenko, V. V. Elizarov. Metrological problems of gas analyzers based on wavelength-scanned cavity ring-down spectroscopy. *Opt. Spectrosc.* **2015**, *118*, 1017.

[31] X. F. Wen, Y. Meng, X. Y. Zhang, X. M. Sun, X. Lee. Evaluating calibration strategies for isotope ratio infrared spectroscopy for atmospheric $^{13}CO_2$ / $^{12}CO_2$ measurement. *Atmos. Meas. Tech.* **2013**, *6*, 1491.

[32] C. Rella. *Accurate stable carbon isotope ratio measurements with rapidly varying carbon dioxide concentrations using the Picarro $\delta^{13}CO_2$ G2101-i gas analyzer*, Picarro Inc., Sunnyvale, California, USA, **2010**.

[33] K. Malowany, J. Stix, A. Van Pelt, G. Lucic. $H_2S$ interference on $CO_2$ isotopic measurements using a Picarro G1101-i cavity ring-down spectrometer. *Atmos. Meas. Tech.* **2015**, *8*, 4075.

[34] S. Bode, R. Fancy, P. Boeckx. Stable isotope probing of amino sugars - a promising tool to assess microbial interactions in soils. *Rapid Commun. Mass Spectrom.* **2013**, *27*, 1367.

[35] G. Tcherkez, R. Bligny, E. Gout, A. Mahé, M. Hodges, G. Cornic. Respiratory metabolism of illuminated leaves depends on $CO_2$ and $O_2$ conditions. *Proc. Natl. Acad. Sci. USA* **2008**, *105*, 797.

[36] A. J. Midwood, P. Millard. Challenges in measuring the $\delta^{13}C$ of the soil surface $CO_2$ efflux. *Rapid Commun. Mass Spectrom.* **2011**, *25*, 232.

[37] D. L. Phillips, J. W. Gregg. Uncertainty in source partitioning using stable isotopes. *Oecologia* **2001**, *127*, 171.

[38] L. Galatry. Simultaneous Effect of Doppler and Foreign Gas Broadening on Spectral Lines. *Phys. Rev.* **1961**, *122*, 1218.

[39] C. Stowasser, A. D. Farinas, J. Ware, D. W. Wistisen, C. Rella, E. Wahl, E. Crosson, T. Blunier. A low-volume cavity ring-down spectrometer for sample-limited applications. *Appl. Phys. B* **2014**, *116*, 255.

[40] C. W. Rella, J. Hoffnagle, Y. He, S. Tajima. Local and regional scale measurements of $CH_4$, $\delta^{13}CH_4$, $C_2H_6$ in the Uintah Basin using a mobile stable isotope analyzer. *Atmos. Meas. Tech.* **2015**, *8*, 4539.

[41] J. Hoffnagle. *Understanding the G2131-i isotopic carbon dioxide data log*, Picarro Inc., Santa Clara, California, USA, **2015**.

[42] J. Hoffnagle. *Understanding the data log created by the G1101-i/G2101-i/G2131-i/G2121-i / G2201-i isotopic carbon dioxide analyzers*, Picarro Inc., Santa Clara, California, USA, **2015**.

[43] L. S. Rothman, I. E. Gordon, Y. Babikov, A. Barbe, D. Chris Benner, P. F. Bernath, M. Birk, L. Bizzocchi, V. Boudon, L. R. Brown, A. Campargue, K. Chance, E. A. Cohen, L. H. Coudert, V. M. Devi, B. J. Drouin, A. Fayt, J. M. Flaud, R. R. Gamache, J. J. Harrison, J. M. Hartmann, C. Hill, J. T. Hodges, D. Jacquemart, A. Jolly, J. Lamouroux, R. J. Le Roy, G. Li, D. A. Long, O. M. Lyulin, C. J. Mackie, S. T. Massie, S. Mikhailenko, H. S. P. Müller, O. V. Naumenko, A. V. Nikitin, J. Orphal, V. Perevalov, A. Perrin, E. R. Polovtseva, C. Richard, M. A. H. Smith, E. Starikova, K. Sung, S. Tashkun, J. Tennyson, G. C. Toon, V. G. Tyuterev, G. Wagner. The HITRAN2012 molecular spectroscopic database. *J. Quant. Spectrosc. Radiat. Transfer* **2013**, *130*, 4.

[44] *HITRAN on the web.* http://hitran.iao.ru, Accessed: 28 May 2016.

[45] R. A. Werner, W. A. Brand. Referencing strategies and techniques in stable isotope ratio analysis. *Rapid Commun. Mass Spectrom.* **2001**, *15*, 501.

[46] International Organization for Standardization. *ISO 6142:2001 Gas analysis - Preparation of calibration gas mixtures*, International Organization for Standardization (ISO), Geneva, Switzerland, **2001**.

[47] Joint Committee for Guides in Metrology. *JCGM 100:2008 Evaluation of measurement data — Guide to the expression of uncertainty in measurement*, International Committee for Weights and Measures (BIPM) / International Electrotechnical Commission (IEC) / International Federation of Clinical Chemistry and Laboratory Medicine (IFCC) / International Laboratory Accreditation Cooperation (ILAC) / International Organization for Standardization (ISO) / International Union of Pure and Applied Chemistry (IUPAC) / International Union of

Pure and Applied Physics (IUPAP) / International Organization of Legal Metrology (OIML), **2008**.

[48] J. Buldyreva, M. Chrysos. Semiclassical modeling of infrared pressure-broadened linewidths: A comparative analysis in $CO_2$–Ar at various temperatures. *J. Chem. Phys.* **2001**, *115*, 7436.

[49] D. C. Benner, C. E. Miller, V. M. Devi. Constrained multispectrum analysis of $CO_2$–Ar broadening at 6227 and 6348 $cm^{-1}$. *Can. J. Phys.* **2009**, *87*, 499.

[50] T. Hikida, K. M. T. Yamada. $N_2$- and $O_2$-broadening of $CO_2$ for the (3001)III←(0000) band at 6231$cm^{-1}$. *J. Mol. Spectrosc.* **2006**, *239*, 154.

[51] C. B. Suárez, F. P. Valero. Intensities, self-broadening, and broadening by Ar and $N_2$ for the 301 III←000 band of $CO_2$ measured at different temperatures. *J. Mol. Spectrosc.* **1978**, *71*, 46.

[52] F. Thibault, B. Calil, J. Buldyreva, M. Chrysos, J. M. Hartmann, J. P. Bouanich. Experimental and theoretical $CO_2$–Ar pressure-broadening cross sections and their temperature dependence. *Phys. Chem. Chem. Phys.* **2001**, *3*, 3924.

[53] R. R. Gamache, J. Lamouroux, A. L. Laraia, J.-M. Hartmann, C. Boulet. Semiclassical calculations of half-widths and line shifts for transitions in the 30012←00001 and 30013←00001 bands of CO2, I: Collisions with $N_2$. *J. Quant. Spectrosc. Radiat. Transfer* **2012**, *113*, 976.

[54] J. Lamouroux, R. R. Gamache, A. L. Laraia, J.-M. Hartmann, C. Boulet. Semiclassical calculations of half-widths and line shifts for transitions in the 30012←00001 and 30013←00001 bands of $CO_2$ II: Collisions with $O_2$ and air. *J. Quant. Spectrosc. Radiat. Transfer* **2012**, *113*, 991.

[55] R. R. Gamache, J. Lamouroux. The vibrational dependence of half-widths of $CO_2$ transitions broadened by $N_2$, $O_2$, air, and $CO_2$. *J. Quant. Spectrosc. Radiat. Transfer* **2013**, *117*, 93.

[56] F. P. J. Valero, C. B. Suarez. Measurement at different temperatures of absolute intensities, line half-widths, and broadening by Ar and $N_2$ for the 3001II←0000 band of $CO_2$. *J. Quant. Spectrosc. Radiat. Transfer* **1978**, *19*, 579.

[57] D. A. Long, L. Gameson, G. W. Truong, K. Bielska, A. Cygan, J. T. Hodges, J. R. Whetstone, R. D. van Zee. The Effects of Variations in Buffer Gas Mixing Ratios on Commercial Carbon Dioxide Cavity Ring-Down Spectroscopy Sensors. *J. Atmos. Oceanic Technol.* **2013**, *30*, 2604.

[58] H. Nara, H. Tanimoto, Y. Tohjima, H. Mukai, Y. Nojiri, K. Katsumata, C. W. Rella. Effect of air composition ($N_2$, $O_2$, Ar, and $H_2O$) on $CO_2$ and $CH_4$ measurement by wavelength-scanned cavity ring-down spectroscopy: calibration and measurement strategy. *Atmos. Meas. Tech.* **2012**, *5*, 2689.

[59] S. Nakamichi, Y. Kawaguchi, H. Fukuda, S. Enami, S. Hashimoto, M. Kawasaki, T. Umekawa, I. Morino, H. Suto, G. Inoue. Buffer-gas pressure broadening for the (3 0(0) 1)III <-- (0 0 0) band of $CO_2$ measured with continuous-wave cavity ring-down spectroscopy. *Phys. Chem. Chem. Phys.* **2006**, *8*, 364.

[60] A. Predoi-Cross, W. Liu, C. Holladay, A. V. Unni, I. Schofield, A. R. W. McKellar, D. Hurtmans. Line profile study of transitions in the 30012←00001 and 30013← 00001 bands of carbon dioxide perturbed by air. *J. Mol. Spectrosc.* **2007**, *246*, 98.

[61] A. Predoi-Cross, A. R. W. McKellar, D. C. Benner, V. M. Devi, R. R. Gamache, C. E. Miller, R. A. Toth, L. R. Brown. Temperature dependences for air-broadened Lorentz half-width and pressure shift coefficients in the 30013←00001 and 30012←00001 bands of $CO_2$ near 1600 nm. *Can. J. Phys.* **2009**, *87*, 517.

[62] M. Krystek, M. Anton. A weighted total least-squares algorithm for fitting a straight line. *Meas. Sci. Technol.* **2007**, *18*, 3438.

[63] R Core Team. *R: A Language Environment for Statistical Computing*, R Foundation for Statistical Computing, Vienna, Austria, **2015**.

[64] C. Zhu, R. H. Byrd, P. Lu, J. Nocedal. Algorithm 778: L-BFGS-B: Fortran subroutines for large-scale bound-constrained optimization. *ACM Trans. Math. Softw.* **1997**, *23*, 550.

[65] C. Y. Kwok, O. Laurent, A. Guemri, C. Philippon, B. Wastine, C. W. Rella, C. Vuillemin, F. Truong, M. Delmotte, V. Kazan, M. Darding, B. Lebegue, C. Kaiser, I. Xueref-Remy, M. Ramonet. Comprehensive laboratory and field testing of cavity ring-down spectroscopy analyzers measuring $H_2O$, $CO_2$, $CH_4$ and CO. *Atmos. Meas. Tech.* **2015**, *8*, 3867.

| Standard ID | Gravimetric values | | | | | | | PBE adjustments | | PBE corrected values (G2131-i apparent) | | | | |
|---|---|---|---|---|---|---|---|---|---|---|---|---|---|---|
| | $C^{16}O_2$ (ppm) | $^{12}C^{16}O_2$ (ppm) | $^{13}C^{16}O_2$ (ppm) | $R_{CO_2}$* | $\delta^{13}$C-$CO_2$ (‰)** | *x* $N_2$ | *x* $O_2$ | $^{12}C^{16}O_2$ (ppm) | $^{13}C^{16}O_2$ (ppm) | $C^{16}O_2$ (ppm) | $^{12}C^{16}O_2$ (ppm) | $^{13}C^{16}O_2$ (ppm) | $R_{CO_2}$* | $\delta^{13}$C-$CO_2$ (‰)** |
| LE1 | 426.17 ± 0.18 | 401.10 ± 0.19 | 25.07 ± 0.14 | 6.25 ± 0.04 | +4591 ± 31 | 0.7896 | 0.2099 | -0.80 ± 0.07 | -0.04 ± 0.02 | 425.33 ± 0.26 | 400.30 ± 0.26 | 25.03 ± 0.16 | 6.25 ± 0.04 | +4594 ± 36 |
| LE2 | 497.64 ± 0.43 | 397.49 ± 0.51 | 100.15 ± 0.62 | 25.20 ± 0.18 | +21536 ± 163 | 0.7901 | 0.2094 | -0.83 ± 0.07 | -0.16 ± 0.08 | 496.65 ± 0.52 | 396.66 ± 0.58 | 99.99 ± 0.71 | 25.21 ± 0.20 | +21547 ± 181 |
| TT | 1049.42 ± 0.25 | 999.50 ± 0.27 | 49.92 ± 0.25 | 4.99 ± 0.03 | +3467 ± 23 | 0.7893 | 0.2097 | -2.01 ± 0.18 | -0.08 ± 0.04 | 1047.33 ± 0.43 | 997.49 ± 0.45 | 49.84 ± 0.30 | 5.00 ± 0.03 | +3469 ± 27 |
| HE1 | 2048.41 ± 0.27 | 2023.00 ± 0.26 | 25.41 ± 0.02 | 1.256 ± 0.001 | +123.6 ± 1.1 | 0.7872 | 0.2107 | -3.68 ± 0.33 | -0.04 ± 0.02 | 2044.69 ± 0.60 | 2019.31 ± 0.59 | 25.38 ± 0.04 | 1.257 ± 0.002 | +124.1 ± 2.0 |
| HE2 | 2102.64 ± 0.42 | 2002.92 ± 0.47 | 99.72 ± 0.51 | 4.98 ± 0.03 | +3453 ± 23 | 0.7872 | 0.2107 | -3.66 ± 0.33 | -0.14 ± 0.08 | 2098.84 ± 0.76 | 1999.26 ± 0.80 | 99.58 ± 0.59 | 4.98 ± 0.03 | +3455 ± 27 |
| NA1 | 490 ± 5 | 484.4 ± 4.8 | 5.22 ± 0.05 | 1.0780† ± 0.0003 | -35.8† ± 0.3 | ambient air‡ | | - | | As per gravimetric values: no PBE adjustment as background gas compositions were that of ambient air‡ | | | | |
| NA2 | 1024 ± 10 | 1013 ± 10 | 11.0 ± 0.1 | 1.0875† ± 0.0003 | -27.3† ± 0.3 | ambient air‡ | | - | | | | | | |
| ZERO | < 0.10 | < 0.10 | < 0.005 | - | - | ambient air‡ | | - | | | | | | |

* $R_{CO_2}$ ($^{13}CO_2/^{12}CO_2$) data are scaled by $10^2$ for ease of comprehension

** $\delta^{13}$C-$CO_2$ values are reported against VPDB[45]

† IRMS value

‡ $x$N$_2$ = 0.781, $x$O$_2$ = 0.209, $x$Ar = 0.010 (from Friedrichs et al.[29])

**Table 1. Composition data of standards used for calibrating the G2131-i. Details of the PBE (pressure broadening effect) adjustments are set out in Supporting Information 2 (see also text). ± values denote uncertainties resulting from gravimetric preparation, PBE adjustment, and their combination (except for the $R_{CO_2}$ and $\delta^{13}$C-$CO_2$ data for standards NA1 and NA2 where their ± values are the IRMS measurement uncertainties).**

| Calibration model | | Model parameters | | | | | | Total weighted residual squares | Partial $r^2$ |
|---|---|---|---|---|---|---|---|---|---|
| | | $x^{12}CO_2$ (Eq. 1 or 8) | | | | $x^{13}CO_2$ (Eq. 2) | | | |
| | | $A_{12}$ | $B_{12}$ | $C_{12}$ | $D_{12}$ | $A_{13}$ | $B_{13}$ | | |
| **$x^{12}CO_2$ linear** (Eq. 1) | WLS solution | -0.618 | 1.6661 | - | - | -0.020 | 0.6291 | 110.81 | n/a |
| | Oxygen isotope corrected solution * | -0.618 | 1.6742 | - | - | -0.020 | 0.6323 | | |
| | Standard error on parameter estimate | 0.015 | 0.0002 | - | - | 0.004 | 0.0002 | | |
| **$x^{12}CO_2$ non-linear** (Eq. 8) | WLS solution | -0.639 | 1.677 | 0.0095 | -6.32 | -0.020 | 0.6280 | 8.82 | 0.92 |
| | Oxygen isotope corrected solution * | -0.639 | 1.685 | 0.0095 | -6.29 | -0.020 | 0.6310 | | |
| | Standard error on parameter estimate | 0.015 | 0.002 | 0.0010 | 1.25 | 0.004 | 0.0003 | | |

* The WLS solution was adjusted so calibrated data include all isotopologues of $^{12}CO_2$ and $^{13}CO_2$, not only the $^{12}C^{16}O_2$ and $^{13}C^{16}O_2$ directly measured by CRDS. The ratio of $CO_2/C^{16}O_2$ at natural abundance $^{17}O$ and $^{18}O$ is 1.004878

**Table 2. Results from weighted least squares (WLS) optimisation of calibration models applied to G2131-i measurements of standard gases.**

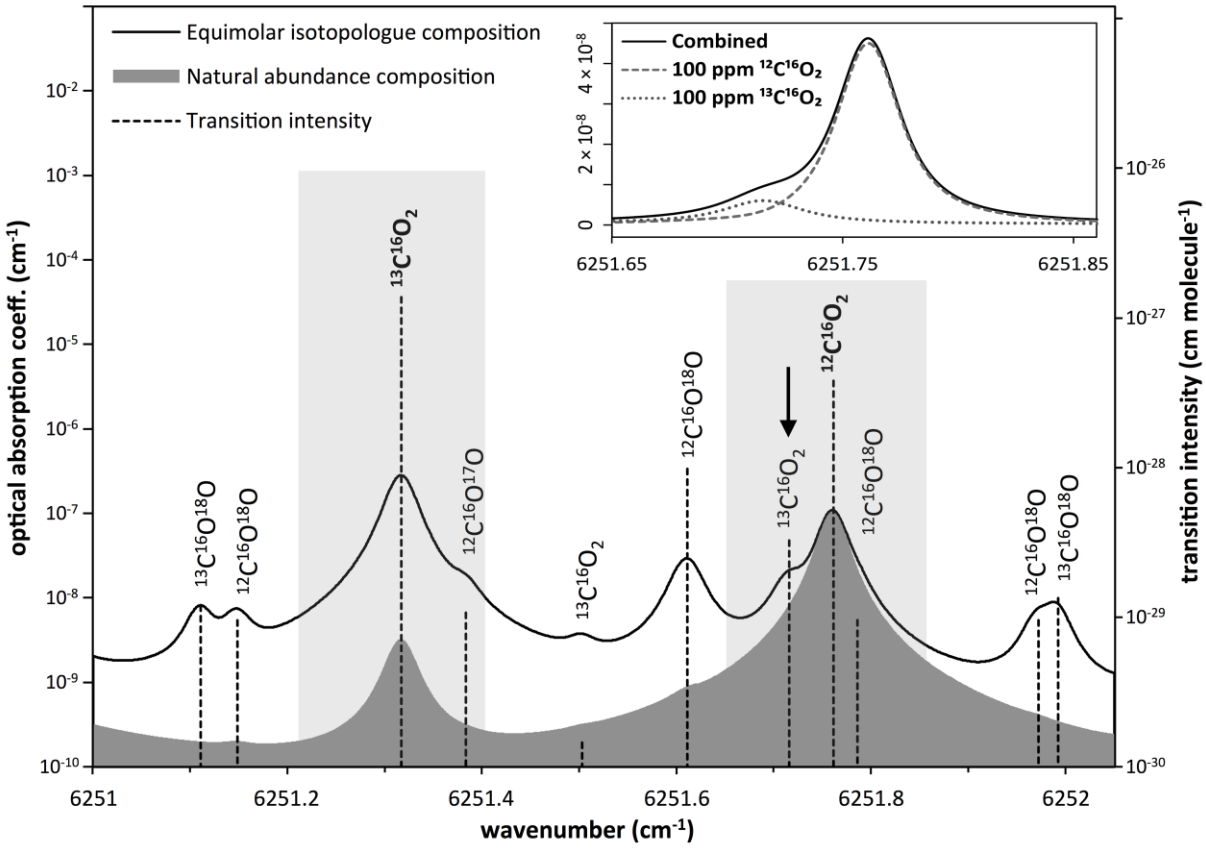


Figure 1. HITRAN[43] generated spectral simulations[44] of $CO_2$ in air (0.184 atm, 318.15 K) across the G2131-i measurement region. Total absorption spectra for natural abundance and equimolar compositions of $CO_2$ isotopolouges are presented (each normalised to 100 ppm $^{12}C^{16}O_2$), with transition intensities and centres overlaid. Shaded columns indicate the G2131-i scanning ranges for the R(12) $^{13}C^{16}O_2$ and R(36) $^{12}C^{16}O_2$ bands (bold labels, respectively centred at 6151.315 and 6151.760 cm$^{-1}$). A close-up (inset) of the R(36) $^{12}C^{16}O_2$ spectral region illustrates the potential for interference from the shouldering R(10) $^{13}C^{16}O_2$ transition (arrow, main plot; 6251.716 cm$^{-1}$) at high fractions of $^{13}CO^2$ (equimolar composition shown). Note the logarithmic and linear y-axes.

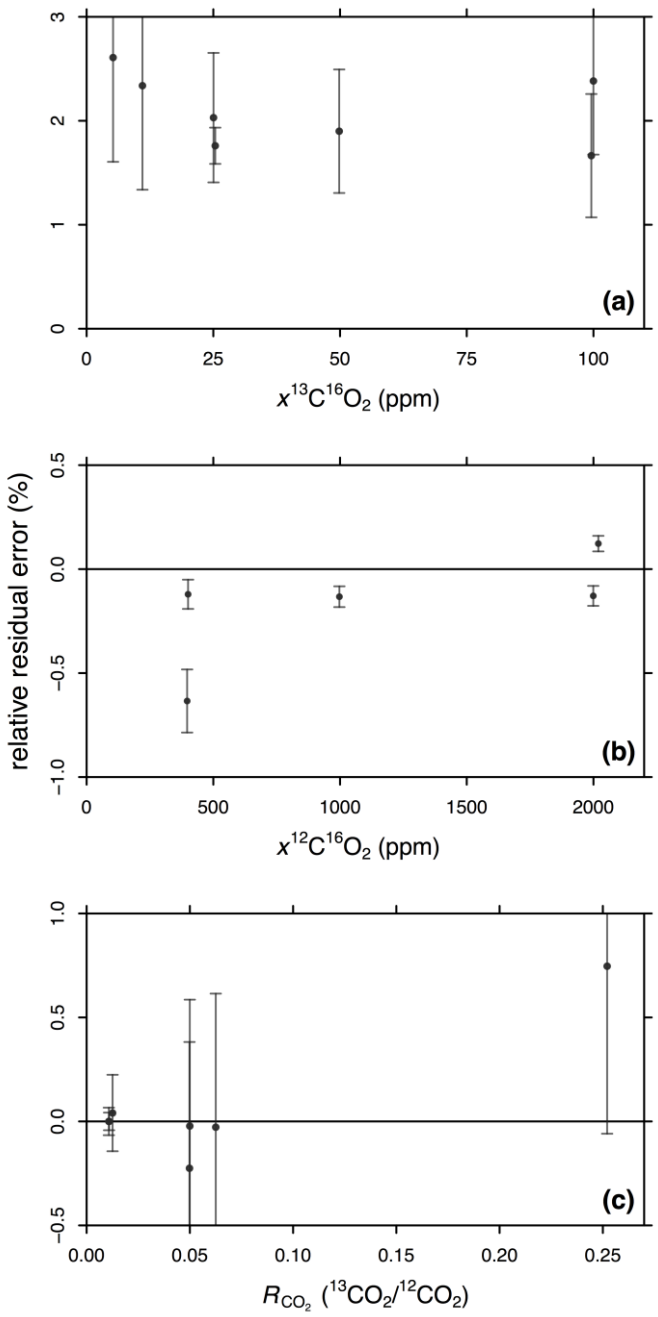


Figure 2. Relative errors of G2131-i measurements (raw reported values) of standard gases for (a) $x^{13}C^{16}O_2$, (b) $x^{12}C^{16}O$, and (c) $^{13}C/^{12}C$ isotope ratio ($R_{CO2}$). Error bars denote the combined uncertainty of the PBE adjusted gravimetric standard value and measurement precision.

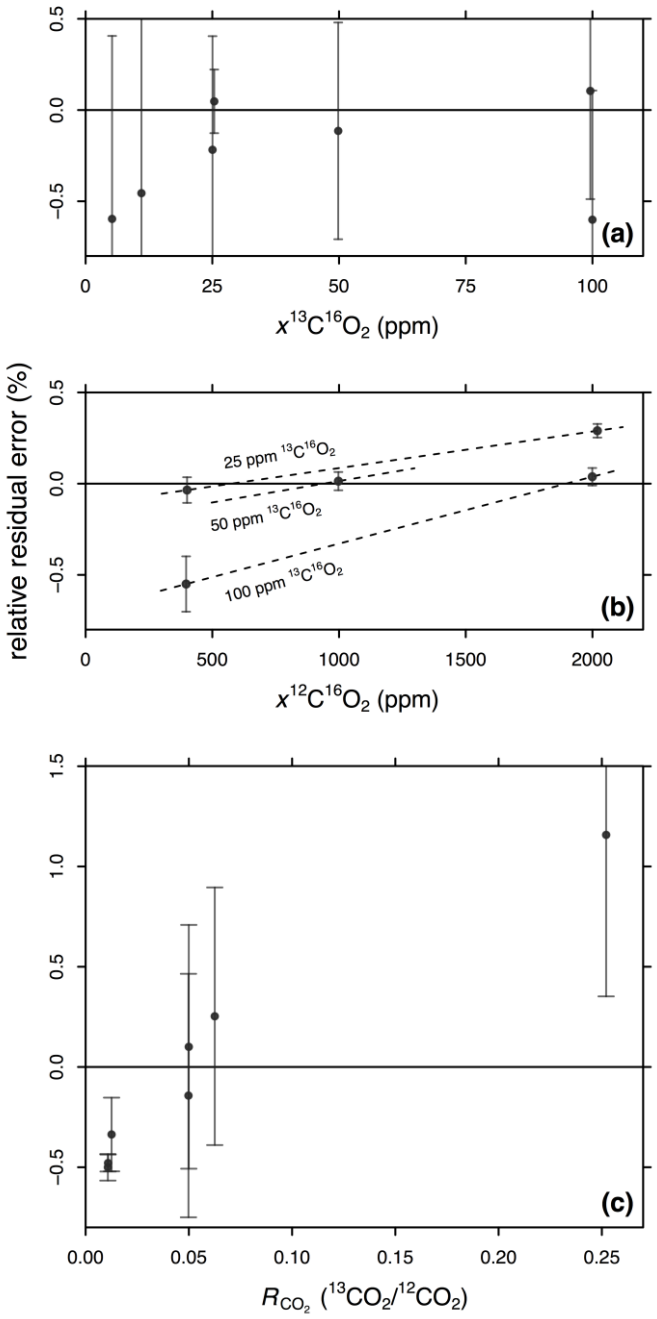


Figure 3. Residual errors from applying a linear calibration model (Eq. 1-4) to G2131-i spectral measurements of standard gases for (a) $x^{13}C^{16}O_2$, (b) $x^{12}C^{16}O$, and (c) $^{13}C/^{12}C$ isotope ratio ($R_{CO2}$). Error bars denote the combined uncertainty of the PBE adjusted gravimetric value and measurement precision.

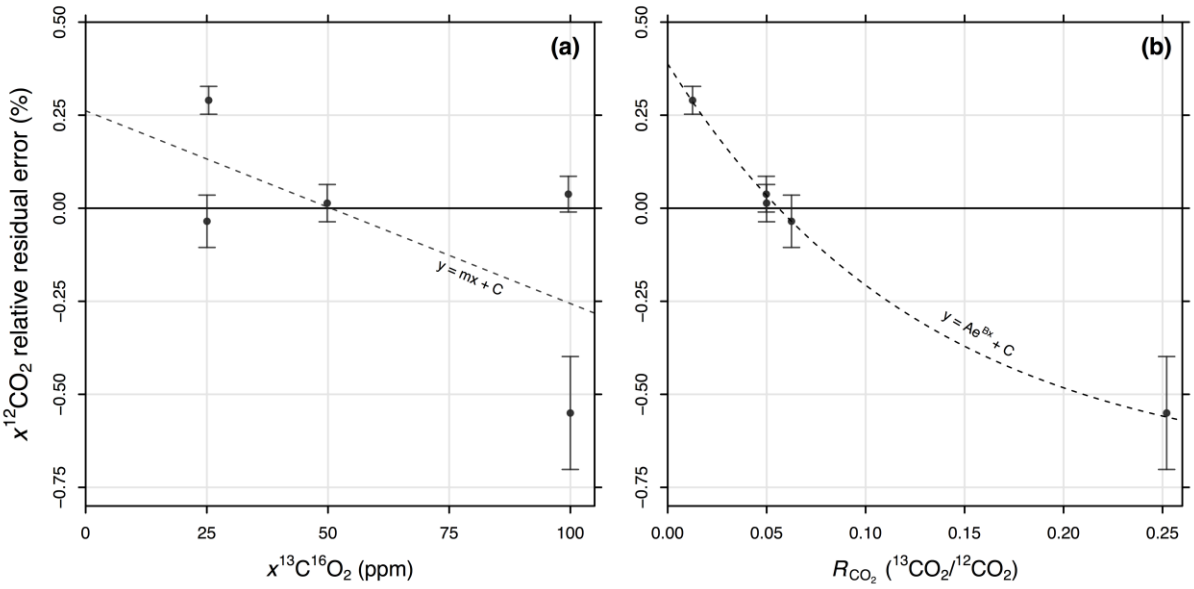


Figure 4. Residual errors in $x^{12}CO_2$ from the linear calibration model (Fig. 3b) as a function of gravimetric values of (a) $x^{13}C^{16}O_2$ mole fraction and (b) $^{13}C/^{12}C$ isotope ratio ($R_{CO2}$). Error bars denote the combined uncertainty of the PBE adjusted gravimetric value and measurement precision. Dashed lines denote least squares fitted functions. Data from standards NA1, NA2, and ZERO omitted for clarity.

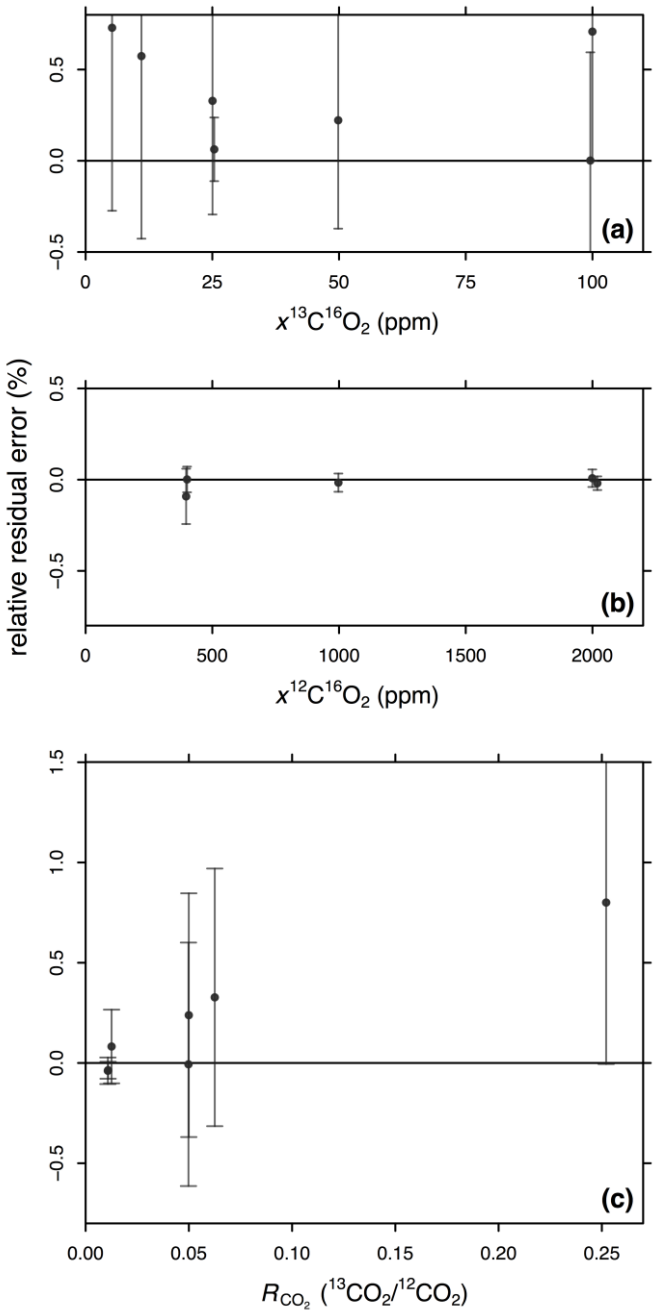


Figure 5. Residual errors from applying the WLS optimised non-linear calibration model (Eq. 2-4, 8) to G2131-i spectral measurements of standard gases for (a) $x^{13}C^{16}O_2$, (b) $x2^3C^{16}O_2$, and (c) $^{13}C/^{12}C$ isotope ratio ($R_{CO2}$). Error bars denote the combined uncertainty of the PBE adjusted gravimetric value and measurement precision.

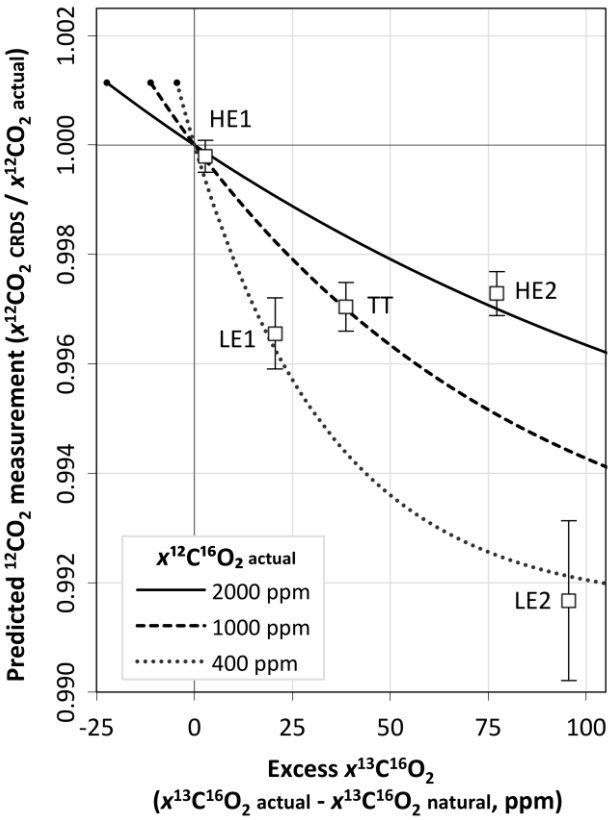


Figure 6. Predicted effect on $^{12}CO_2$ measurements from varying $x^{13}C^{16}O_2$ when using a G2131-i CRDS analyser linearly calibrated by $CO_2$ standards with natural isotope abundances (i.e. $R_{CO2} \approx R_{VPDB}$). Excess $x^{13}C^{16}O_2$ is the increase in $x^{13}C^{16}O_2$ compared to the natural abundance level that corresponds to the $^{12}CO_2$ mole fraction. Derived from comparing our non-linear calibration (Eqs. 7, 8) to an ordinary linear model (Eq. 1), addition of $^{13}CO_2$ (e.g. $_{13}$C-enrichment) is predicted to decrease the reported CRDS measurement due to interference on the baseline of the $^{12}CO_2$ spectral feature. Actual measurements of our $^{13}$C-enriched standards (Table 1) are overlaid (square symbols, labelled) to indicate the parameter space covered by our calibration (error bars are the PBE adjusted gravimetric uncertainties).